sjst.scst.edu.ly

Surman Journal for Science and Technology

مجلة صرمان للعلوم والتقنية

ISSN: Online (2790-5721) - Print (2790-5713)

Vol 6, No.2, Jun - Dec. 2024

Pages: 103 ~ 120

DYNAMIC ANALYSIS OF A CRACKED BEAM UNDER MOVING LOAD BASED ON MODIFIED ADOMIAN DECOMPOSITION METHOD

[1]Naseradin Abujnah, [2]Nizar Ramadan

[1]Department of Industry Engineering, College of Engineering Technology, Messallata, Libya
[2]Department of Mechanical Engineering, Surman College for Science and Technology, Libya
[1]naabujnah@ftem.edu.ly
[2]nizar.r@scst.edu.ly

ABSTRACT

It is well known that continuous system motion equations are based on partial differential equations. Their solutions are more difficult than discrete systems' equations of motions, especially if the equations of motions are non-linear. Different efforts have been implemented to solve non-linear partial differential equations for a long time. Researchers have tried to use different methods for this purpose. Modified Adomian Decomposition Method (MADM) is a promising method and has been applied to solve non-linear partial differential equations obtained in engineering systems. In this article, MADM is used to investigate the forced vibration of the Euler-Bernoulli (EB) cracked beams under a moving load. For this purpose, MADM was used to create the mentioned vibration response. This model consists of moving load acting on two continuous segments where the crack is modeled as a rotational spring with sectional flexibility. For this purpose, the equations of motion with a fourth order have been used. They are non-homogenous partial differential equations, which were used for mathematical modeling. Dynamic response was analyzed to understand the cracked supported beam beneath the moving load, which revealed the impact of concentrated force on crack location as well as extension. Some numerical results were presented by using MATLAB software to compute the vibration analysis and plot the deflection. The solution and its methodology were verified with the help of some studies. Results have shown that MADM is effective and accurate for vibration analysis of cracked beams under a moving load.

الملخص

من المعروف أن معادلات حركة النظام المستمرة تعتمد على المعادلات التفاضلية الجزئية. وحلولها أصعب من معادلات الحركات في الأنظمة المنفصلة، خاصة إذا كانت معادلات الحركات غير خطية. لقد تم بذل جهود مختلفة لحل المعادلات التفاضلية الجزئية غير الخطية لفترة طويلة. وقد حاول الباحثون استخدام طرق مختلفة لهذا الغرض. تعد طريقة التحلل الآدومي المعدلة (MADM) طريقة واعدة وتم تطبيقها لحل المعادلات التفاضلية الجزئية غير الخطية التي تم الحصول عليها في الأنظمة الهندسية. في هذه المقالة، تم استخدام الآدومي المعدلة لفحص الاهتزاز القسري للعتبات المتشققة من نوع إويلر – بؤنولي (EB) تحت حمل متحرك. ولهذا الغرض، تم استخدام الآدومي المعدلة لإنشاء استجابة الاهتزاز المذكورة. يتكون هذا النموذج من حمل متحرك يعمل على جزأين متواصلين حيث تم تصميم الشق على شكل زنبرك دوراني يتمتع بمرونة مقطعية. ولهذا الغرض تم استخدام معادلات الحركة من الدرجة الرابعة. وهي معادلات تفاضلية جزئية غير متجانسة، والتي تم استخدامها للنمذجة الرياضية. تم تحليل الاستجابة الديناميكية لفهم الحزمة المدعومة المتشققة أسفل الحمل المتحرك، والتي كشفت عن تأثير القوة المركزة على موقع الشق بالإضافة إلى الامتداد. تم تقديم بعض النتائج العددية باستخدام برنامج الماتلاب (MATLAB) لحساب تحليل الاهتزازات ورسم الانحراف. تم التحقق من الحل ومنهجيته بمساعدة بعض الدراسات. أظهرت النتائج أن الآدومي المعدلة فعالة ودقيقة في تحليل اهتزاز العتبات المتشققة تحت الحمل المتحرك.

Keywords: Modified Adomian Decomposition Method (MADM), crack detection, dynamic response, moving load, Euler Bernoulli beam.

SJST
sjst.scst.edu.ly
Surman Journal for Science and Technology
مجلة صرمان للعلوم والتقنية
ISSN: Online (2790-5721) - Print (2790-5713)
Vol 6, No.2, Jun - Dec. 2024
Pages: 103 ~ 120

1. INTRODUCTION

Vibration of bridges under moving loads is a significant topic and a challenge both for mechanical and structural engineers. Moving load causes substantial deflection and stress when it is compared to a similar static load. Cracks may occur on a bridge as a result of these kinds of stresses. Cracks are the major reason behind bridge structure failures. When a crack initiates in a bridge structure, it loses its stiffness, reducing the lifetime of the bridge structure. It is probable to predict the crack depth and its location based on the changes in vibration parameters. From the earliest days of railroad development during the last century, bridge vibration under a moving load has attracted the attention of numerous researchers [1-13]. (Fryba, 1934) conducted a comprehensive vibration study of a beam under different kinds of moving loads [14]. (Reis et al., 2008) analyzed the bridge structures' dynamic responses under moving loads [15]. (Olsson, 1991) studied the EB beam in situations where it was underneath the moving loads by applying modal analysis using accurate shapes [16]. (Mao, 2012) also studied the uniform cracked EB beams' free vibrations [17]. (Mofid & Shadnam, 2000) analyzed the dynamic responses of EB beneath the movable mass using developed discrete elements [18]. (Parhi and Behera,1997) investigated a damage circular shaft and its dynamic deflection under a moving load applying the Runge-Kutta procedure [19]. (Bilello & Bergman) [8] studied the damaged EB beam responses theoretically and experimentally under the moving loads. They modeled the damage using rotational springs after evaluating their compliance applying mechanics principle of linear elastic fractures. Their analysis was based on an unknown deflection and its series expansion, also called as eigenfunction of a beam. (Esmailzadeh & Ghorashi, 1995) investigated the beam vibration in case of partly distributed uniform moving mass [20]. (Jena & Parhi, 2016) analyzed a cracked cantilever beam and its response to moving load applying continuum mechanics in addition to Duhamel integral [21]. Moreover, (Law & Zhu, 2004) analyzed the cracked concrete bridge, which was subjected to moving loads in the form of vehicles [22]. They studied the dynamic behavior of the cracked bridge through breathing and open crack models. (Mahmoud & Zaid, 2002) also analyzed a simply supported cracked beam with the help of an iterative analysis approach [23]. (Nahvi and Jabbari, 2005) used experimental and FEM approaches to study a crack identification problem [24]. (Lin, 2007) developed his analytical approach to explain the forced responses observed in a simply supported and cracked beam of a moving vehicle [25]. Pala et al. also analyzed a cracked beam's dynamic response underneath the moving load with inserted Coriolis and Centripetal forces using Duhamel integral [26]. (Ariaei et al, 2009) presented the un-damped EB beams' dynamic response in the presence of breathing cracks when moving mass was applied to it with the help of finite element method (FEM) and discrete element technique (DET) [3]. (An et al.,2010) analyzed the impact of a crack on simply supported un-damped beams, which were bearing moving spring-masses [1]. They proposed this technique on the time history, and its spatial wavelet analysis. The time history was practically taken from the real vehicles, which moved on the bridge. They used Adomian decomposition method (ADM) and its modified form of MADM. This method has been recently used for solving differential equations, which were derived to be used in different engineering applications. Solving homogeneous and inhomogeneous differential equations and linear and nonlinear equations is useful to find constant and variable coefficients. The superiority of this method lies on its ability to significantly reduce computations while maintaining the numerical solution accuracy.

sjst.scst.edu.ly

Surman Journal for Science and Technology

مجلة صرمان للعلوم والتقنية

ISSN: Online (2790-5721) - Print (2790-5713)

Vol 6, No.2, Jun - Dec. 2024

Pages: 103 ~ 120

(Bozyigit et al., 2018) studied the impact of foundation damping, modulus of sub-grade reaction, and axial compressive load on the beam model's natural frequencies applying several boundary conditions in the differential transformation method and the Adomian decomposition method, as well as (Mao & Pietrzko, 2012) analyzed the free vibration of the varying section of a simply supported beam using ADM [27]. (Mao & Chen, 2013) analyzed the vibration problem of beams consisting of arbitrary cracks following the ADM and applying boundary conditions and (Mao, 2016) investigated the crack damage detection and free vibrations by applying ADM and EB beam theory [28-29]. (Coskun et al., 2011) used ADM, Variational Iteration Method and Homotropy Perturbation Procedure to analyze vibration of varying-section EB beams and compared the associated mode shapes to their natural frequencies [30]. However, only in one research, (Bilik & Karaçay, 2015) applied MADM to analyze the vibration response of intact bridge subjected to a constant load [8]. They applied MADM to vibration analysis of an intact bridge subjected to concentrated force. Most of the previous studies in this area have used MADM to examine the free vibration of a cracked beam subjected to a moving load, not forced vibration. MADM has been applied first time by this presented study to solution of the equation of motion of the cracked beam subjected to a moving load. Vibration analysis of a cracked simply supported beam subjected to moving load as EB beam has been performed by using MADM. Moving load in the equation of motion with a fourth order was expressed by Dirac Delta function and the second order was transformed into a second order ordinary differential equation considering the non-homogeneous partial differential equation, boundary, and initial conditions.

2. ANALYSIS OF CRACKED BEAMS

In this study, a simply supported and cracked beam that has a length (l), and its open crack was positioned at $x = l_0$. A moving force F with a constant velocity is applied on the beam from its left end to right end. Uniform beam has a cross-section of width-b and height-h. Moreover, at the cross-section a crack depth of $-a$ was formed as seen in Figure (1).

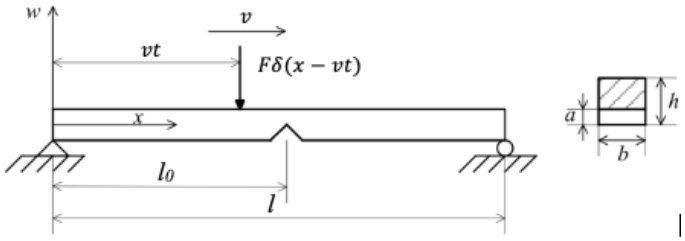

Figure (1): A simply supported cracked beam under moving load.

In Figure (1), the crack has sub-divided the beam into two parts. Considering the EB beam theory, the equation of motion for free vibration of the both parts can be written as follows:

$$EI\frac{\partial^4 w_1}{\partial x^4} + \rho A\frac{\partial^2 w_1}{\partial t^2} = 0, \quad 0 < x < l_0 \tag{1}$$

$$EI\frac{\partial^4 w_1}{\partial x^4} + \rho A\frac{\partial^2 w_1}{\partial t^2} = 0, \quad l_0 < x < l \tag{2}$$

sjst.scst.edu.ly

Surman Journal for Science and Technology

ISSN: Online (2790-5721) - Print (2790-5713)

مجلة صرمان للعلوم والتقنية

Vol 6, No.2, Jun - Dec. 2024

Pages: 103 ~ 120

where w_1 and w_2 are the vertical displacement before and after the crack, respectively. The boundary conditions of a cracked simply supported beam are

$$w_1(0,t) = w_2(l,t) = 0 \quad , \qquad w_1''(0,t) = w_2''(l,t) = 0 \tag{3}$$

the compatibility conditions requirements before and after the crack

$$w_1(l_0^-,t) = w_2(l_0^+,t), w_1''(l_0^-,t) = w_2''(l_0^+,t) \; and \; w_1''(l_0^-,t) = w_2''(l_0^+,t) \tag{4}$$

where the symbols l_0^- and l_0^+indicate the locations promptly prior and next the crack location, respectively. The discontinuity position at $x = l_0$ is considered on the beam by dividing the beam into two parts prior and next the crack. The condition of discontinuity at the crack position for a simply beam can be expressed as

$$w_2(l_0^+,t) = w_1(l_0^-,t) + \left(\frac{EIc}{l_0}\right) l_0 w_2''(l_0^+,t) \tag{5}$$

Here *c* is the local crack flexibility, that can be establish from the following function

$$c = \frac{[6\pi(1-\nu^2)h\phi(\alpha)]}{EI} \tag{6}$$

here $\nu$is Poisson ratio,*h* is height of the beam section and $\alpha$is the crack depth ratio

$$\alpha = \frac{a}{h} \tag{7}$$

and

$$\phi(\alpha) = 0.6272\alpha^2 - 1.04533\alpha^3 + 4.5948\alpha^4 - 9.9736\alpha^5 + 20.2948\alpha^6 - 33.0351\alpha^7 + 47.106\alpha^8 - 40.7556\alpha^9 + 19.6\alpha^{10} \tag{8}$$

The mode shapes of vibration of the two parts of the beam, before and after the crack, respectively, are

$$\varphi_{1s}(x) = a_{1s}\, sin(\lambda x) + b_{1s}\, cos(\lambda x) + c_{1s}\, sinh(\lambda x) + d_{1s} cosh(\lambda x), \quad x < l_0, \text{ s} = 1,2,3\ldots \tag{9}$$

$$\varphi_{2s}(x) = a_{2s} \sin\lambda(x-l_0) + b_{2s} \cos\lambda(x-l_0) + c_{2s} \sinh\lambda(x-l_0) + d_{2s}\cosh\lambda(x-l_0), \qquad l_0 < x < l \text{ , s} = 1,2,3,\ldots \tag{10}$$

$$\lambda = \frac{\rho A \omega_s^2}{EI} \tag{11}$$

Where the coefficients a_{is},b_{is}, c_{is} and d_{is}can be found by substituting previous equations into the boundary condition equations. The two spans boundary conditions are:

$$\varphi_{1s}(0) = 0, \varphi_{1s}''(0) = 0, \varphi_{2s}(l) = 0 \; and \varphi_{2s}''(l) = 0 \tag{12}$$

By using the Equation (9) and (12) b_{1s}, d_{1s} are obtained as follows.

$$b_{1s} = d_{1s} = 0 \tag{13}$$

and

SJST
sjst.scst.edu.ly
Surman Journal for Science and Technology
ISSN: Online (2790-5721) - Print (2790-5713)
مجلة صرمان للعلوم والتقنية
Vol 6, No.2, Jun - Dec. 2024
Pages: 103 ~ 120

$$a_{2s}\sin\lambda(l-l_0)+b_{2s}\cos\lambda(l-l_0)+c_{2s}\sinh\lambda(l-l_0)+d_{2s}\cosh\lambda(l-l_0)=0 \quad (14)$$

$$-a_{2s}\sin\lambda(l-l_0)-b_{2s}\cos\lambda(l-l_0)+c_{2s}\sinh\lambda(l-l_0)+d_{2s}\cosh\lambda(l-l_0)=0 \quad (15)$$

The previous equations can be expressed in a matrix form as following

$$\begin{bmatrix} r_{11}r_{12}r_{13}r_{14} \\ r_{21}r_{22}r_{23}r_{24} \end{bmatrix} \times \begin{bmatrix} a_{2s} \\ b_{2s} \\ c_{2s} \\ d_{2s} \end{bmatrix} = \begin{bmatrix} 0 \\ 0 \end{bmatrix} \quad (16)$$

Here

$$r_{11}=\sin\lambda(l-l_0),\quad r_{12}=\cos\lambda(l-l_0), r_{13}=\sinh\lambda(l-l_0), r_{14}=\cosh\lambda(l-l_0)$$
$$r_{21}=-\sin\lambda(l-l_0), r_{22}=-\cos\lambda(l-l_0), r_{23}=\sinh\lambda(l-l_0)\ and\ r_{24}=\cosh\lambda(l-l_0) \quad (17)$$

Using conditions in Equations (4) and (5) with Equations (9) and (10)

$$\begin{aligned} &a_{1s}\sin(\lambda l_0)+b_{1s}\cos(\lambda l_0)+c_{1s}\sinh(\lambda l_0)+d_{1s}\cosh(\lambda l_0)=d_{2s}+b_{2s} \\ &a_{1s}\sin(\lambda l_0)-b_{s1}\cos(\lambda l_0)+c_{s1}\sinh(\lambda l_0)+d_{1s}\cosh(\lambda l_0)=d_{2s}-b_{2s} \\ &-a_{1s}\cos(\lambda l_0)+b_{1s}\sin(\lambda l_0)+c_{1s}\cosh(\lambda l_0)+d_{1s}\sinh(\lambda l_0)=c_{2s}-a_{2s} \end{aligned} \quad (18)$$

$$a_{1s}\cos(\lambda l_0)-b_{1s}\sin(\lambda l_0)+c_{1s}\cosh(\lambda l_0)+d_{1s}\sinh(\lambda l_0)=c_{2s}+a_{2s+}EIc\lambda(b_{2s}-d_{2s}) \quad (19)$$

$$\begin{bmatrix} s_{11} & s_{12} & s_{13} & s_{14} \\ s_{21} & s_{22} & s_{23} & s_{24} \\ s_{31} & s_{32} & s_{33} & s_{34} \\ s_{41} & s_{42} & s_{43} & s_{44} \end{bmatrix} \begin{bmatrix} a_{1s} \\ b_{1s} \\ c_{1s} \\ d_{1s} \end{bmatrix} = \begin{bmatrix} a_{2s} \\ b_{2s} \\ c_{2s} \\ d_{2s} \end{bmatrix} \quad (20)$$

Where

$$s_{11}=\cos\lambda l_0-\delta\sin\lambda l_0\ , s_{12}=-\sin\lambda l_0-\delta\cos\lambda l_0\ , s_{13}=\delta\sinh\lambda l_0\ , s_{14}=\cosh\lambda l_0$$
$$s_{21}=\sin\lambda l_0\ , s_{22}=\cos\lambda l_0\ , s_{13}=0\ , n_{14}=0 \quad (21)$$
$$s_{31}=-\delta\sin\lambda l_0\ , s_{32}=-\delta\cos\lambda l_0\ , s_{13}=\cosh\lambda l_0+\delta\sinh\lambda l_0\ , s_{14}=\sinh\lambda l_0+\delta\cosh\lambda l_0 \quad (22)$$

and $\delta=\frac{\lambda EIc}{2}$

Substituting Equation (20) into Equation (16) yields

$$\begin{bmatrix} 0 \\ 0 \end{bmatrix} = \begin{bmatrix} r_{11}r_{12}r_{13}r_{14} \\ r_{21}r_{22}r_{23}r_{24} \end{bmatrix} \begin{bmatrix} s_{11} & s_{12} & s_{13} & s_{14} \\ s_{21} & s_{22} & s_{23} & s_{24} \\ s_{31} & s_{32} & s_{33} & s_{34} \\ s_{41} & s_{42} & s_{43} & s_{44} \end{bmatrix} \begin{bmatrix} a_{1s} \\ b_{1s} \\ c_{1s} \\ d_{1s} \end{bmatrix} \quad (23)$$

Or $$\begin{bmatrix} 0 \\ 0 \end{bmatrix} = R_{2\times4} \times S_{4\times4} \begin{bmatrix} a_{1s} \\ b_{1s} \\ c_{1s} \\ d_{1s} \end{bmatrix} = T \times \begin{bmatrix} a_{1s} \\ b_{1s} \\ c_{1s} \\ d_{1s} \end{bmatrix} \quad (24)$$

Where

$$\begin{aligned} t_{11} &= r_{11}s_{11}+r_{12}s_{21}+r_{13}s_{31}+r_{14}s_{41} \\ t_{12} &= r_{11}s_{12}+r_{12}s_{22}+r_{13}s_{32}+r_{14}s_{42} \end{aligned} \quad (25)$$

SJST
sjst.scst.edu.ly
Surman Journal for Science and Technology
مجلة صرمان للعلوم والتقنية
ISSN: Online (2790-5721) - Print (2790-5713)
Vol 6, No.2, Jun - Dec. 2024
Pages: 103 ~ 120

$$t_{13} = r_{11}s_{13} + r_{12}s_{23} + r_{13}s_{33} + r_{14}s_{43}$$
$$t_{14} = r_{11}s_{14} + r_{12}s_{24} + r_{13}s_{34} + r_{14}s_{44}$$
$$t_{21} = r_{21}s_{11} + r_{22}s_{21} + r_{23}s_{31} + r_{24}s_{41}$$
$$t_{22} = r_{21}s_{12} + r_{22}s_{22} + r_{23}s_{32} + r_{24}s_{42}$$
$$t_{23} = r_{21}s_{13} + r_{22}s_{23} + r_{23}s_{33} + r_{24}s_{43}$$
$$t_{24} = r_{21}s_{14} + r_{22}s_{24} + r_{23}s_{34} + r_{24}s_{44}$$

The existence of nontrivial solutions requires that the value of the following determinant is zero

$$\begin{vmatrix} r_{11} & r_{13} \\ r_{21} & r_{23} \end{vmatrix} = 0 \tag{26}$$

The eigenvalues are results of the previous determinant after that the natural frequencies of the cracked beam can be obtained analytically by substituting eigenvalues in Equation (11).
By using Equations (13), (14), (15), (16) and (17), the coefficients can be written as follows.

$$\begin{cases} c_{1s} = \dfrac{a_{1s}\left(\delta \sin(\lambda l_0)\sinh\left(\lambda(l-l_0)\right)\right)}{\sinh\left(\lambda(l-l_0)\right)\left(\cosh(\lambda l_0) + \delta\sinh(\lambda l_0)\right) + \cosh\left(\lambda(l-l_0)\right)\sinh(\lambda l_0)} \\ a_{2s} = a_{1s}(\cos(\lambda l_0) - \delta\sin(\lambda l_0)) + \cosh\left(\lambda(l-l_0)\right)\sinh(\lambda l_0) \\ b_{2s} = a_{1s} sin(\lambda l_0) \\ c_{2s} = c_{1s}\left(\cosh(\lambda l_0) + \delta\sinh(\lambda l_0)\right) - a_{1s}\delta\sin(\lambda l_0) \\ d_{2s} = c_{1s}\sin h(\lambda l_0) \end{cases} \tag{27}$$

all the values of coefficients depend on the value of a_{1s}

$$\varphi_{1s}(x) = a_{1s}(\sin(\lambda x) + z\sinh(\lambda x)), \qquad 0 < x < l_0 \tag{28}$$

$$\varphi_{s2}(x) = a_{s1}\Big((\cos(\lambda l_0) - \delta\sin(\lambda l_0)) + z\delta\sinh(\lambda l_0)\sin\lambda(x-l_0) + \sin(\lambda l_0)\cos\lambda(x-l_0) + z\left(\cosh(\lambda l_0) + \delta\sinh(\lambda l_0)\right) - \delta\sin(\lambda l_0)\sinh\lambda(x-l_0) + z\sinh(\lambda l_0)\cosh\lambda(x-l_0)\Big), \quad l_0 < x < l \tag{29}$$

Where

$$z = \frac{(\delta\sin(\lambda l_0)\sinh(\lambda(l-l_0))}{\sinh\left(\lambda(l-l_0)\right)\left(\cosh(\lambda l_0) + \delta\sinh(\lambda l_0)\right) + \cosh(\lambda(l-l_0))\sinh(\lambda l_0)} \tag{30}$$

There is only one unknown coefficient a_{1s} in the Eigen functions equations, Equation (28) and Equation (29), can be found it by using orthonormality condition:

$$\|\varphi_s(x)\| = \sqrt{\int_0^l \varphi_s^2(x)dx} = \left(\int_0^{l_1} \varphi_{s_{1s}}^2(x)dx + \int_{l_1}^{l} \varphi_{2s}^2(x)dx\right)^{1/2} = 1 \tag{31}$$

a_{1s} can be obtained by using Equations (28), (29) and (31) as

sjst.scst.edu.ly

Surman Journal for Science and Technology

ISSN: Online (2790-5721) - Print (2790-5713)

مجلة صرمان للعلوم والتقنية

Vol 6, No.2, Jun - Dec. 2024

Pages: 103 ~ 120

$$a_{1s} = \left(\frac{1}{\int_0^{l_0} \varphi_{1s}^2(x)dx + \int_{l_0}^{l} \varphi_{2s}^2(x)dx} \right)^{1/2} \quad (32)$$

3. THE PRINCIPLE OF MADM

MADM has been used in recent years for solving partial differential equations, which are highly complex, and widely used in mathematics, physics and engineering applications. Their modified and rendered forms give very useful outcomes [31-32] .The second order non-homogeneous equation, according to this method and its initial conditions, has been expressed as follows:

$$w''(t) + P(t)w' + N(t) = g(t), \qquad w(0) = k_0 \text{and} \qquad w'(0) = k_1 \quad (33)$$

Where N(t) is nonlinear function, P(t) and g(t) are given functions, and k_0 and k_1 are constants. According to MADM, the new differential operator L is given below:

$$L = e^{-\int P(t)dt} \frac{d}{dt}\left(e^{\int P(t)dt} \frac{d}{dt}\right) \quad (34)$$

If P (t) = 0, Equation 33 can be rewritten as:

$$Lw = g(t) - N(t) \quad (35)$$

In this method, the inverse of the operator L has been applied a two-fold integral operator.

$$L^{-1}(\cdot) = \int_0^t e^{-\int P(t)dt} \int_0^t e^{\int P(t)dt} (\cdot)dtdt \quad (36)$$

By applying L^{-1}on Equation (35) becomes as follow:

$$w(t) = \mathrm{k}_0 + \mathrm{k}_1 t + L^{-1}g(t) - L^{-1}N(t) \quad (37)$$

4. THE MATHEMATICAL MODEL OF THE BEAM SUBJECTED TO MOVING LOADS

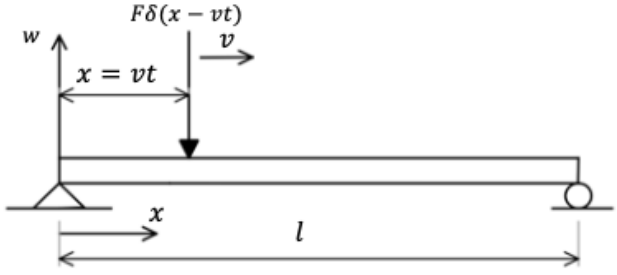

Figure (2): A Simply supported beam under moving loads

SJST
sjst.scst.edu.ly
Surman Journal for Science and Technology
مجلة صرمان للعلوم والتقنية
ISSN: Online (2790-5721) - Print (2790-5713)
Vol 6, No.2, Jun - Dec. 2024
Pages: 103 ~ 120

Fig. 2 shows a simply supported and the moving load. As the force travels from left to right direction of the beam ends, it is assumed that the beam vibrates only in w-direction. Neglecting the shear force, rotary inertia and damping effects, the equation of motion for the beam under load F can be defined as:

$$EI\frac{\partial^4 w(x,t)}{\partial x^4}+\rho A\frac{\partial^2 w(x,t)}{\partial t^2}=F\delta(x-vt) \quad ,0<x<l \tag{38}$$

With boundary and initial conditions:

$$w(0,t)=0,\frac{\partial^2 w(0,t)}{\partial x^2}=0 \ ,w(l,t)=0 \ ,\frac{\partial^2 w(l,t)}{\partial x^2}=0\,,\ \ w(x,0)=0\,,\ \frac{\partial w(x,0)}{\partial t}=0 \tag{39}$$

Here:
EI = flexural rigidity.
w (x, t) = vertical displacement
m = Constant mass of beam per unit length
F = moving load with constant velocity v
δ = Dirac delta function
The series solution can be expressed as given below

$$w(x,t)=\sum_{s=1}^{S}\varphi_s(x)\eta_s(t) \tag{40}$$

Here $\varphi_s(x)$ and $\eta_s(t)$ represent eigenfunctions and generalized coordinates of the system, respectively, while S represents repetitions needed to achieve a solution [33]. By substituting Equation 40 in Equation 38, and then, integrating it from 0 to l after multiplying by $\varphi_m(x)$ then it yields

$$\sum_{s=1}^{S}\left[\frac{d^2\eta_s(t)}{dt^2}+{\omega_s}^2\eta_s(t)\right]\int_0^l\varphi_s(x)\varphi_m(x)\,dx=\int_0^l\frac{F}{\rho A}\delta(x-vt)\,\varphi_m(x)dx \tag{41}$$

Recalling the following condition of orthogonality and properties of Dirac delta functions.

$$\int_0^l\varphi_s(x)\,\varphi_m(x)dx=\begin{cases}0\,, & s\neq m\\ \frac{l}{2}\,, & s=m\end{cases} \quad and \int\delta(\tau-\tau_0)\,f(\tau)=f(\tau_0) \tag{42}$$

and substituting the Equation (42) into Equation (41) leads to

$$\frac{d^2\eta_s(t)}{dt^2}+{\omega_s}^2\eta_s(t)=\frac{2F}{l\rho A}\varphi_s(vt) \tag{43}$$

where

$$\omega_s=\left(\frac{n\pi x}{l}\right)^2\sqrt{\frac{EI}{\rho A}} \tag{44}$$

SJST
sjst.scst.edu.ly
Surman Journal for Science and Technology
مجلة صرمان للعلوم والتقنية
ISSN: Online (2790-5721) - Print (2790-5713)
Vol 6, No.2, Jun - Dec. 2024
Pages: 103 ~ 120

For the intact simply supported beam, the assumed mode shape may be written as

$$\varphi_s(x) = sin\left(\frac{n\pi x}{l}\right) \quad (45)$$

The cracked beam

In this study, a simply supported cracked beam with length l was considered. The crack was located at the location $x = l_0$ as shown in Figure 1. A force F moved along the beam at a constant velocity v. A movement took place from left to right. The crack divided the beam into two segments. For a cracked beam, $\varphi_s(x)$ represents the mode shapes of the two segments of the beam, which is defined by equations 9 and 10.

Since the nature of eigenfunctions is orthogonal; therefore, it will be expressed as:

$$\int_0^l {\varphi_m}^2 dx = \int_0^l {\varphi_s}^2\, dx = \int_0^{l_0} {\varphi_{1s}}^2\, dx + \int_{l_0}^l {\varphi_{2s}}^2\, dx \quad (46)$$

By applying the orthogonal relation between the shapes of the mode, Equation 6 will become:

$$\frac{d^2\eta_s(t)}{dt^2} + {\omega_s}^2\eta_s(t) = \begin{cases} F_z[a_{1s}\, sin(\varepsilon t) + b_{1s}\, cos(\varepsilon t) + c_{1s}\, sinh(\varepsilon t) + d_{1s} cosh(\varepsilon t)], & t \le \dfrac{l_0}{v} \\ F_z[a_{2s} \sin(\varepsilon t - \theta) + b_{2s} \cos(\varepsilon t - \theta) + c_{2s} \sinh(\varepsilon t - \theta) + d_{2s}\cosh(\varepsilon t\ - \theta)], & t > \dfrac{l_0}{v} \end{cases} \quad (47)$$

where

$$\varepsilon = \lambda v, \theta = \lambda l_0 \text{ and } F_z = \frac{F}{\rho A}$$

5. MADM FOR CRACKED BEAM (WITH MOVING LOAD)

The first segment of the beam can be expressed by the following equation:

$$\frac{d^2\eta_{1s}(t)}{dt^2} + {\omega_s}^2\eta_s(t) = \frac{F}{\rho A}[a_{1s}\, sin(\lambda x) + b_{1s}\, cos(\lambda x) + c_{1s}\, sinh(\lambda x) + d_{1s} cosh(\lambda x)], \quad t \le \frac{l_0}{v} \quad (48)$$

For solving equation given above using MADM, it is imperative to introduce L^{-1} operator on both sides. The solution will be as follows:

$$\sum_{s=0}^{\infty} \eta_s(t) = k_0 + k_1 t - L^{-1}[{\omega_s}^2\eta_s(t) - F_z[a_{1s}\, sin(\varepsilon t) + b_{1s}\, cos(\varepsilon t) + c_{1s}\, sinh(\varepsilon t) + d_{1s} cosh(\varepsilon t)] \quad (49)$$

Under zero initial conditions, the solution of Equation (38) has the form:

$$\eta_{1s}(t) = \frac{a_{1s}F_z}{\varepsilon^2 - {\omega_s}^2}\left[\frac{\varepsilon}{\omega_s} sin(\omega_s t) - sin(\varepsilon t)\right] - \frac{c_{1s}\, F_z}{\varepsilon^2 + {\omega_s}^2}\left[\frac{\varepsilon}{\omega_s} sin(\omega_s t) - sinh(\varepsilon t)\right] \quad (50)$$

In the same manner, for $t > \frac{l_0}{v}$ the solution can be found by applying same MADM procedure

SJST
sjst.scst.edu.ly
Surman Journal for Science and Technology
ISSN: Online (2790-5721) - Print (2790-5713)
مجلة صرمان للعلوم والتقنية
Vol 6, No.2, Jun - Dec. 2024
Pages: 103 ~ 120

For the second segment of beam Equation (47) becomes

$$\frac{d^2\eta_s(t)}{dt^2} + {\omega_s}^2\eta_s(t) = F_z[a_{2s}\sin(\varepsilon t-\theta) + b_{2s}\cos(\varepsilon t-\theta) + c_{2s}\sinh(\varepsilon t-\theta) + d_{2s}\cosh(\varepsilon t-\theta)], \quad t > \frac{l_0}{v} \tag{51}$$

For solving equation given above using the MADM introducing the L^{-1} operator on both sides, the solution can be written after the operation as

$$\sum_{r=0}^{\infty}\eta_r(t) = k_0 + k_1 t - L^{-1}[{\omega_s}^2\eta_s(t) - F_z[a_{2s}\sin(\varepsilon t-\theta) + b_{2s}\cos(\varepsilon t-\theta) + c_{2s}\sinh(\varepsilon t-\theta) + d_{2s}\cosh(\varepsilon t-\theta)] \tag{52}$$

Considering the MADM,$\eta_0(t)$ is assumed to be of the following form

$$\eta_0(t) = k_0 + k_1 t + L^{-1}F_z[a_{2s}\sin(\varepsilon t-\theta) + b_{2s}\cos(\varepsilon t-\theta) + c_{2s}\sinh(\varepsilon t-\theta) + d_{2s}\cosh(\varepsilon t-\theta)] \tag{53}$$

and the repetition relation for $\eta_{r+1}(t)$

$$\eta_{r+1}(t) = -L^{-1}[{\omega_s}^2\eta_r(t)], \text{ r=0,1,2,3…} \tag{54}$$

Using the same procedure as the previous it yields

$$\begin{aligned}\eta_{2s}(t) = \bar{a}_{2s}&\left[\frac{\varepsilon}{\omega_s}cos\theta\sin(\omega_s t) - \sin\theta\cos(\omega_s t) + sin(\theta-\varepsilon t)\right] \\ &+ \bar{b}_{2s}\left[\frac{\varepsilon}{\omega_s}\sin\theta\sin(\omega_s t) + \cos\theta\cos(\omega_s t) - \cos(\theta-\varepsilon t)\right] \\ &- \bar{c}_{2s}\left[\frac{\varepsilon}{\omega_s}cosh\,\theta\,sin(\omega_s t) - sinh\,\theta\cos(\omega_s t) + \sinh(\theta-\varepsilon t)\right] \\ &+ \bar{d}_{2s}\left[\frac{\varepsilon}{\omega_s}sinh\,\theta\,sin(\omega_s t) - cosh\,\theta\cos(\omega_s t) + \cosh(\theta-\varepsilon t)\right] + k_0 cos(\omega_s t) \\ &+ \frac{k_1}{\omega_s}sin(\omega_s t)\end{aligned} \tag{55}$$

It can be easily shown that the coefficients in Equation (55) are in the forms

$$\bar{a}_{2s} = \frac{a_{2s}F_z}{\varepsilon^2-{\omega_s}^2}, \quad \bar{b}_{2s}, \frac{b_{2s}F_z}{\varepsilon^2-{\omega_s}^2}, \quad \bar{c}_{2s} = \frac{c_{2s}F_z}{\varepsilon^2+{\omega_s}^2}, \quad \bar{d}_{2s} = \frac{d_{2s}F_z}{\varepsilon^2+{\omega_s}^2} \tag{56}$$

To determine k_0 and k_1 in Equation (55), the initial conditions are used

$$\eta_{1s}\left(\frac{l_0}{v}\right) = \eta_{2s}\left(\frac{l_0}{v}\right) = H\left(\frac{l_0}{v}\right) + k_0 cos\left(\frac{\omega_s l_0}{v}\right) + \frac{k_1}{\omega_s}sin\left(\frac{\omega_s l_0}{v}\right) \tag{57}$$

And

$$\dot{\eta}_{1s}\left(\frac{l_0}{v}\right) = \dot{\eta}_{n2s}\left(\frac{l_0}{v}\right) = \dot{H}\left(\frac{l_0}{v}\right) - k_0\omega_s\, sin\left(\frac{\omega_s l_0}{v}\right) + k_1 cos\left(\frac{\omega_s l_0}{v}\right) \tag{58}$$

SJST
sjst.scst.edu.ly
Surman Journal for Science and Technology
مجلة صرمان للعلوم والتقنية
ISSN: Online (2790-5721) - Print (2790-5713)
Vol 6, No.2, Jun - Dec. 2024
Pages: 103 ~ 120

where

$$H(t) = \bar{a}_{2s}\left[\frac{\varepsilon}{\omega_s}cos\theta\,\sin(\omega_s t) - \sin\theta\cos(\omega_s t) + sin(\theta - \varepsilon t)\right] + \bar{b}_{2s}\left[\frac{\varepsilon}{\omega_s}\sin\theta\,\sin(\omega_s t) + \cos\theta\,\cos(\omega_s t) - \cos(\theta - \varepsilon t)\right] - \bar{c}_{2s}\left[\frac{\varepsilon}{\omega_s}cosh\,\theta\,sin(\omega_s t) - sinh\,\theta\,cos(\omega_s t) + sinh(\theta - \varepsilon t)\right] + \bar{d}_{2s}\left[\frac{\varepsilon}{\omega_s}sinh\,\theta\,sin(\omega_s t) - cosh\,\theta\,\cos(\omega_s t) + cosh(\theta - \varepsilon t)\right] \quad (59)$$

k_0 can be written as follows from Equation (57) and Equation (58)

$$k_0 = \frac{\eta_{1s}\left(\frac{l_0}{v}\right) - H\left(\frac{l_0}{v}\right) - \frac{k_1}{\omega_s}sin\left(\frac{\omega_s l_0}{v}\right)}{cos\left(\frac{\omega_s l_0}{v}\right)} \quad (60)$$

and

$$k_0 = \frac{\dot{H}\left(\frac{l_0}{v}\right) - \dot{\eta}_{1s}\left(\frac{l_0}{v}\right) + k_1 cos\left(\frac{\omega_s l_0}{v}\right)}{\omega_s\,sin\left(\frac{\omega_s l_0}{v}\right)} \quad (61)$$

Subtracting Equation (61) from Equation (60) yields

$$k_1 = \left[\eta_{1s}\left(\frac{l_0}{v}\right) - H\left(\frac{l_0}{v}\right)\right]\omega_s\,\sin\left(\frac{\omega_s l_0}{v}\right) + \left[\dot{\eta}_{1s}\left(\frac{l_0}{v}\right) - \dot{H}\left(\frac{l_0}{v}\right)\right]\cos\left(\frac{\omega_s l_0}{v}\right) \quad (62)$$

Substitution of Equation (62) in Equation (60) yields

$$k_0 = cos\left(\frac{\omega_s l_0}{v}\right)\left(\eta_{1s}\left(\frac{l_0}{v}\right) - H\left(\frac{l_0}{v}\right)\right) - \left(\dot{\eta}_{1s}\left(\frac{l_0}{v}\right) - \dot{H}\left(\frac{l_0}{v}\right)\right)\frac{sin\left(\frac{\omega_s l_0}{v}\right)}{\omega_s} \quad (63)$$

A very important point here is that the Equation (50) is the answer of Equation (47) before the load passes over the crack and when the load passes over the crack then the Equation (55) is the answer of Equation (47), respectively.

6. VALIDITY OF THE PRESENT SOLUTION

Investigations were carried out to test the efficiency and accuracy of MADM solutions. They were investigated by comparing the results of the studies in literature. It is possible to reduce the present solutions (for a cracked beam) to the corresponding results of an intact beam by reducing the crack depth ratio to 0; therefore, we can compare it with intact beams. (Karoumi, 1998) investigated a simply supported intact beam, which was under a moving load. Indeed, the result proposed by [34] can be easily verified if $\alpha = 0$. For further validation of the obtained solutions, they were compared to the reference values [35]. Figure 3 shows the first comparison of the present results, which was matched with those obtained in Karoumi's study (1998) [34], in which, the system parameters were taken from the same study. We showed the computation by the simplified analysis method for mid-span deflection. In addition, the second comparison of the present results was matched with those obtained in a study by [35], as shown in Figure 4.

sjst.scst.edu.ly

Surman Journal for Science and Technology

مجلة صرمان للعلوم والتقنية

ISSN: Online (2790-5721) - Print (2790-5713)

Vol 6, No.2, Jun - Dec. 2024

Pages: 103 ~ 120

Moreover, the system parameters were taken from the paper mentioning the computations by the Green Function Method for mid-span deflection. Both the comparisons were done using the same MATLAB coding of the present method. Excellent agreement between the obtained values and the reference values was found.

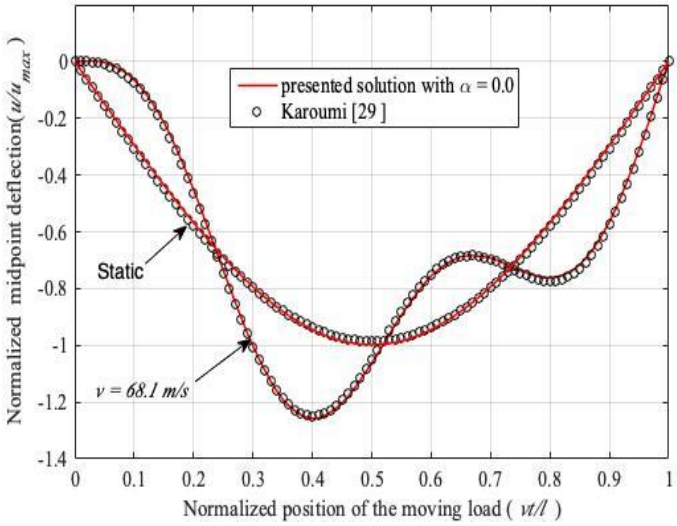

Figure (3): Comparison of the results of the presented study with Karoumi for cracked simply supported beam under moving load when $\alpha = 0$

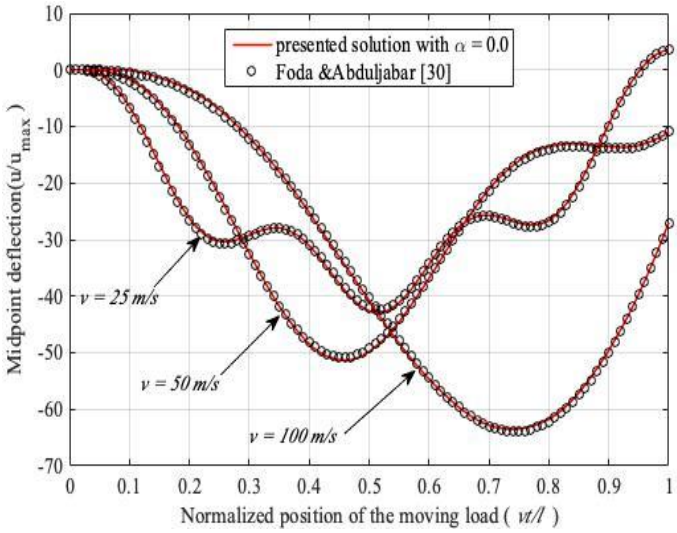

Figure (4): Comparison of the results of the presented study with Foda & Abduljabbar for cracked simply supported beam under moving load when $\alpha = 0$

7. NUMERICAL EXAMPLES

In this research, MADM was applied to a simply supported cracked beam, which was subjected to a moving load. The material and geometrical parameters of used beam are: Young's modulus E= 210 GPa, Length l= 20 m, width b= 0.2 m, height h =0.2 m, Poisson's ratio ν= 0.3, and density ρ = 7860 kg/m^3. It was observed that the beam had a maximum deflection at the

sjst.scst.edu.ly

Surman Journal for Science and Technology

مجلة صرمان للعلوم والتقنية

ISSN: Online (2790-5721) - Print (2790-5713)

Vol 6, No.2, Jun - Dec. 2024

Pages: 103 ~ 120

midpoint where the load was applied. That midpoint showed two types of deflection: dynamic and static, which is shown in the previous and the following graphs in order to explain the two phenomenon. This value is given by $w_{max} = \frac{Fl^3}{48EI}$where the moving load represents F=9810 N. First of all, it is necessary to determine the position of the dynamic deflections and the effect of the crack depth. For this purpose, the normalized position of the moving load (vt/l) and the normalized midpoint deflection (w/w_{max}) were plotted for several crack depth ratios (α), which is shown in Figure 5. In this case, the crack occurred at the midpoint; so, the normal deflections of the midpoint increased with increasing crack depth. In Figure 6, the normalized moving load position vs. the normalized midpoint deflection have been plotted for different crack locations, which are $0.3l$, $0.5l$ and$0.7l$. When a crack is located at some distance from the midpoint, it reduces the normalized midpoint deflection, and the maximum normalized deflection point is displaced in the direction of the crack location. Looking closely at Figures 5 and 6, it is obvious that the normalized deflection is affected by crack depth ratio instead of the crack position. Figure 7 shows the normalized dynamic response at the mid-span of cracked beam for various moving load velocities (5,15, 25, 35, and 45 m/s) with $\alpha = 0.5$. As expected, increasing the moving load velocity results in a maximum mid-span deflection, which is dynamic in nature because the velocity becomes closer to the critical velocity (28 m/s). At that point, the velocity is almost 62% of the critical velocity. After that, the normalized dynamic mid-span maximum deflection starts decreasing with its maximum deflection position shifting towards the right side until it reaches the end of the beam. Figure 8 shows the moving loads and the dynamic deflection response, which was exerted on the cracked simply supported beam at its mid-point with $\alpha = 0.5$. In this case, the constant velocity of the moving load was *v=5 m/s*. It is obvious that when the load was increased from 5 to 45 *kN*, the normalized beam mid-point deflection increased. Table 1 shows the effects of crack depth and its location on the natural frequency of a cracked beam under a moving load. It can be seen that when the crack depth was increased from 0.25 mm to 0.7 mm, the natural frequency of cracked beam under moving load decreased. Also, it is obvious that when the crack location shifted away from the mid-point, it reduced the natural frequency of cracked beam under a moving load.

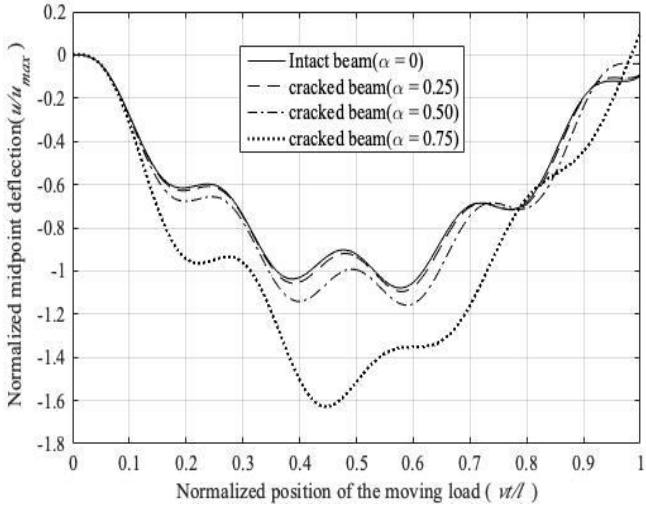

Figure (5): The effect of crack depth ratio on the deflection at mid-span of cracked simply supported beam subjected to moving load with constant velocity (*v* =5m/s) by using MADM.

sjst.scst.edu.ly

Surman Journal for Science and Technology

مجلة صرمان للعلوم والتقنية

ISSN: Online (2790-5721) - Print (2790-5713)

Vol 6, No.2, Jun - Dec. 2024

Pages: 103 ~ 120

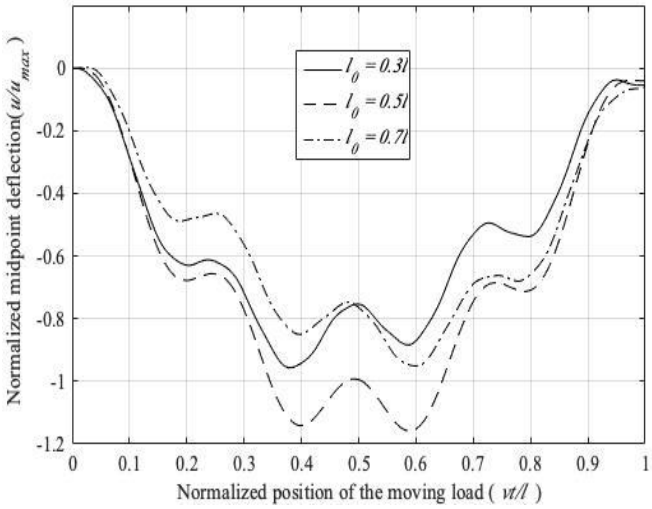

Figure (6): The effect of crack location on the deflection at mid-span of cracked simply supported beam subjected to moving load with constant velocity (v=5m/s) by using MADM.

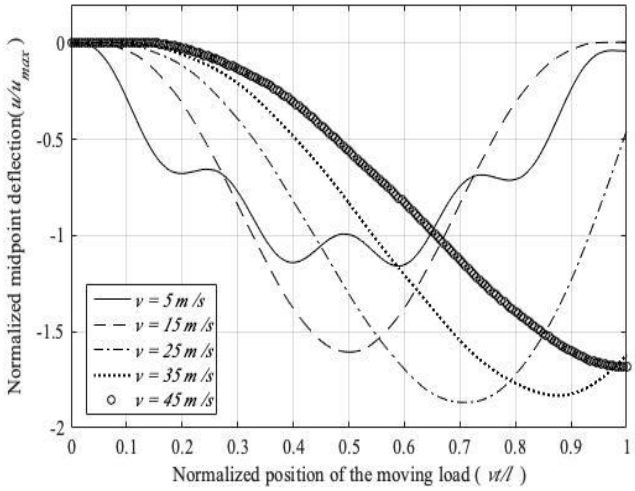

Figure (7): The effect of the moving load velocity (5,15,25,35,45 m/s) on the deflection at mid-span of cracked simply supported beam subjected to moving load by using MADM.

sjst.scst.edu.ly

Surman Journal for Science and Technology

ISSN: Online (2790-5721) - Print (2790-5713)

مجلة صرمان للعلوم والتقنية

Vol 6, No.2, Jun - Dec. 2024

Pages: 103 ~ 120

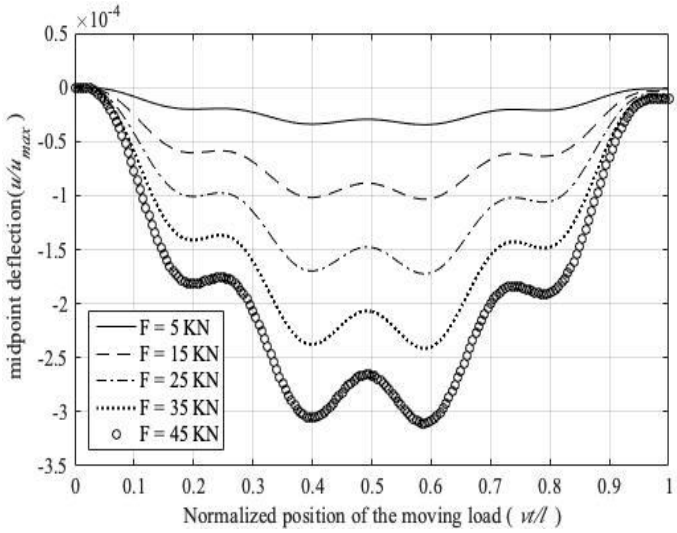

Figure (8): The effect of the amplitude of moving load on the deflection at mid-span of cracked simply supported beam subjected to moving load with constant velocity (v=5m/s) by using MADM.

Table (1) depicts the natural frequencies observed in twelve studied cases. In case when the beam is intact, we used Equation (53) to calculate the first four natural frequencies: ω_1 = 491.20 rad/s, ω_2 = 1964.8 rad/s, ω_3 = 4420.8 rad/s, and ω_4 = 7859.3 rad/s. The obtained frequencies are mentioned in Table 1. It has been observed that the changes in the natural frequency mainly occur because of crack existence, sizes of the cracks and their locations. It is also seen that the cracked beams' natural frequencies reduce when the crack depth increases at the same crack location.

Table (1): The effects of crack depth and its location on the natural frequency of cracked beam under moving load.

Case number	Crack location (l_0)	Crack depth ratio (α)	Natural frequency (rad/s)				Maximum mid-point deflection (cm)
			ω_1	ω_2	ω_3	ω_4	
1	0.3l	0.25	7.29	29.13	65.85	116.90	5.30
2		0.40	7.24	28.85	65.79	116.46	5.46
3		0.55	7.12	28.26	65.65	115.56	5.84
4		0.70	6.82	26.95	65.35	113.50	6.83
5	0.5l	0.25	7.30	29.28	65.50	117.13	6.50
6		0.40	7.20	29.30	64.81	117.13	6.67
7		0.55	7.03	29.28	63.40	117.13	7.02
8		0.70	6.60	29.28	60.35	117.13	8.44
9	0.7l	0.25	7.29	29.28	60.35	117.13	5.37
10		0.40	7.24	28.85	65.79	116.46	5.50
11		0.55	7.12	28.26	65.65	115.56	5.78
12		0.70	6.82	26.95	65.35	113.50	6.60

sjst.scst.edu.ly

Surman Journal for Science and Technology

مجلة صرمان للعلوم والتقنية

ISSN: Online (2790-5721) - Print (2790-5713)

Vol 6, No.2, Jun - Dec. 2024

Pages: 103 ~ 120

8. CONCLUSIONS

In this paper, the cracked beams dynamic response under moving load was first time analyzed by applying MADM. A crack was modeled by rotational massless spring. This article also presents the formulation of the normalized dynamic mid-point deflection of a cracked beam subjected to moving load. Applied method was validated when the obtained values were compared to the values mentioned in some studies, which were found in literature. It was found that the results of MADM have good agreement with the results in literature. The crack depth ratio (α) also showed effect on beam deflection. The results show that when the crack depth ratio is increased, the cracked beam deflection increases as well. Increasing the moving load velocity increases dynamic mid-span maximum deflection. It also increases the maximum mid-point deflection, which shifts to the right side of the beam. Increasing the moving load velocity increases dynamic mid-span maximum deflection. It also increases the maximum mid-point deflection, which shifts to the right end of the beam. Investigation was carried out to understand the impact of crack location on a midpoint beam deflection. It is obvious that when the crack location shifted away from the mid-point, it reduced deflections. The moving load amplitude affected the deflection at the mid-span of simply supported cracked beam. The investigation showed that when the amplitude of the moving load was increased, the cracked beam deflection increased as a consequence. Also, the effects of crack depth and its location on the natural frequency of a cracked beam under a moving load have been investigated. It was shown by this study that a strong mathematical method (MADM) can be used for the cracked beams dynamic response under moving load. In this study, MADM investigated only for one crack. There is a need to study a beam with two or more cracks for a beam under the moving load by using MADM.

REFERENCES

1. An, N., Xia, H., & Zhan, J. (2010). Identification of beam crack using the dynamic response of a moving spring-mass unit. Interaction and Multiscale Mechanics, 3(4), 321–331.
2. (Ramadan, Tur et al. 2017, Ramadan, Tur et al. 2017, Ramadan and ALFARES 2020, Ramadan and Boghdadi 2020, Ramadan and ali Osman 2021, Ramadan, Khalifa et al. 2021, Abubaker, Ramadan et al. 2023, Ramadan, Embaia et al. 2023)
3. Ariaei, A., Ziaei-Rad, S., & Ghayour, M. (2009). Vibration analysis of beams with open and breathing cracks subjected to moving masses. Journal of Sound and Vibration., 326(3), 709.
4. Abubaker, S. S., N. R. Ramadan, S. A. Sultan and M. R. Budar (2023). "Investigation Of The Effect Of Temperature And Time Of Case Hardening On The Mechanical Properties And Microstructure Of Low Carbon Steel (Aisi 1020)." Surman Journal of Science and Technology 5(2): 028-036.
5. Ramadan, N. and H. ALFARES (2020). "Optimize and Improve of The Welding Nugget in The Resistance Welding Process of Carbon Steel by Means of Surface Response Method." Surman Journal of Science and Technology 2(3): 018-007.
6. Ramadan, N. and K. ali Osman (2021). "Isothermal Transformation Temperatures and Its Effect in Hardiness of Pearlite Eutectic Steels R350HT Rails." Surman Journal of Science and Technology 3(1): 028-036.
7. Bilello, C., & Bergman, L. A. (2004). Vibration of damaged beams under a moving mass: Theory and experimental validation. Journal of Sound and Vibration, 274(3–5), 567–582.
8. Bilik, F., & Karaçay, T. (2015). Kuvvet Uygulanmış Basit Mesnetli Euler-Bernoulli Kirişinin Madm Kullanılarak Titreşim Analizi.

9. Ramadan, N. and A. Boghdadi (2020). "Parametric optimization of TIG welding influence on tensile strength of dissimilar metals SS-304 and low carbon steel by using Taguchi approach." Am. J. Eng. Res 9(9): 7-14.
10. Ramadan, N., M. M. Embaia and H. M. Elhamrouni (2023). "Laser Beam Welding Effect On The Microhardness Of Welding Area Of 304 Stainless Steel & Low Carbon Steel." Surman Journal of Science and Technology 5(1): 018-030.
11. Ramadan, N., S. G. Khalifa and H. A. Moftah (2021). "The Influence of the Quality of Libyan Banks' Services on Achieving Customer Satisfaction." Surman Journal of Science and Technology 3(1): 037-046.
12. Ramadan, N., K. Tur and E. Konca (2017). "Design and Simulation of an Apparatus for the Post-Weld Controlled Accelerated Cooling of R350HT Head Hardened Rail Joints."
13. Ramadan, N., K. Tur and E. Konca (2017). "Process design optimization for welding of the head hardened R350 Ht rails and their fatigue: a literature review." International Journal of Engineering Research and Development: 2278-2800.
14. Frỳba, L. (n.d.). Vibration of solids and structures under moving loads. 1999. Noordhoff, Groningen.
15. Reis, M., Pala, Y., & Karadere, G. (2008). Dynamic analysis of a bridge supported with many vertical supports under moving load. The Baltic Journal of Road and Bridge Engineering, 3(1), 14–20.
16. Olsson, M. (1991). On the fundamental moving load problem. Journal of Sound and Vibration, 145(2), 299–307.
17. Mao, Qibo, & Pietrzko, S. (2012). Free vibration analysis of a type of tapered beams by using Adomian decomposition method. Applied Mathematics and Computation, 219(6), 3264–3271.
18. Mofid, M., & Shadnam, M. (2000). On the response of beams with internal hinges, under moving mass. Advances in Engineering Software, 31(5), 323–328.
19. Parhi, D. R., & Behera, A. K. (1997). Dynamic deflection of a cracked shaft subjected to moving mass. Transactions of the Canadian Society for Mechanical Engineering, 21(3), 295–316.
20. Esmailzadeh, E., & Ghorashi, M. (1995). Vibration analysis of beams traversed by uniform partially distributed moving masses. Journal of Sound and Vibration, 184(1), 9–17.
21. Jena, S. P., & Parhi, D. R. (2016). Response of damaged structure to high speed mass. Procedia Engineering, 144, 1435–1442.
22. Law, S. S., & Zhu, X. Q. (2004). Dynamic behavior of damaged concrete bridge structures under moving vehicular loads. Engineering Structures, 26(9), 1279–1293.
23. Mahmoud, M. A., & Abou Zaid, M. A. (2002). Dynamic response of a beam with a crack subject to a moving mass. Journal of Sound and Vibration, 256(4), 591–603.
24. Nahvi, H., & Jabbari, M. (2005). Crack detection in beams using experimental modal data and finite element model. International Journal of Mechanical Sciences, 47(10), 1477–1497.
25. Lin, H.-P. (2007). Vibration analysis of a cracked beam subjected to a traveling vehicle. Proceedings of the 14th International Congress on Sound and Vibration, Cairns, Australia, 9–12.
26. Pala, Y., & Reis, M. (2013). Dynamic response of a cracked beam under a moving mass load. Journal of Engineering Mechanics, 139(9), 1229–1238.
27. Mao Q. (2016). Vibration analysis of cracked beams using Adomian decomposition method and non-baseline damage detection via high-pass filters. Int. J. Acoust. Vibr. International Journal of Acoustics and Vibrations, 21(2), 170–177.
28. Mao, Q, & Chen, X. (2013). Application of adomian decomposition method to free vibration analysis of multi-cracked beams. 20th International Congress on Sound and Vibration 2013, ICSV 2013, 2, 1017–1024.
29. Mao, Qibo. (2012). Free Vibration Analysis of Uniform Beams with Arbitrary Number of Cracks by using Adomian Decomposition Method. World Applied Sciences Journal, 1(19), 1721–1723.

ISSN: Online (2790-5721) - Print (2790-5713)

Vol **6**, No.**2**, Jun - Dec. 2024

Pages: 103 ~ 120

30. Coskun, S. B., Atay, M. T. & Öztürk, B. (2011). Transverse vibration analysis of Euler Bernoulli Beams using analytical approximate techniques, Advances in Vibration Analysis Research, Dr. Farzad Ebrahimi (Ed.), ISBN: 978-953-307-209-8, InTech, Available from: http://www.intechopen.com/books/advances-in-vibration-analysis-research/transverse-vibration-analysis-ofeuler-bernoulli-beams-using-analytical-approximate-techniques
31. Hosseini, M. M., & Nasabzadeh, H. (2006). On the convergence of Adomian decomposition method. Applied Mathematics and Computation, 182(1), 536–543.
32. Hosseini, M. M., & Nasabzadeh, H. (2007). Modified Adomian decomposition method for specific second order ordinary differential equations. Applied Mathematics and Computation, 186(1), 117–123.
33. Ding, H., Chen, L.-Q., & Yang, S.-P. (2012). Convergence of Galerkin truncation for dynamic response of finite beams on nonlinear foundations under a moving load. Journal of Sound and Vibration, 331(10), 2426–2442.
34. Karoumi, R. (1998). Response of cable-stayed and suspension bridges to moving vehicles: Analysis methods and practical modeling techniques [PhD Thesis]. KTH Royal Institute of Technology.
35. Foda, M. A., & Abduljabbar, Z. (1998). A dynamic Green function formulation for the response of a beam structure to a moving mass. Journal of Sound and Vibration, 210(3), 295–306.
36. Hakan Gökdağ. (2013). A Crack Identification Method for Bridge Type Structures under Vehicular Load Using Wavelet Transform and Particle Swarm Optimization. Advances in Acoustics and Vibration, 2013.